Libertas Academica
FREEDOM TO RESEARCH

ORIGINAL RESEARCH

# Diffusion Tensor Metric Measurements as a Function of Diffusion Time in the Rat Central Nervous System

Jonathan D. Thiessen[1,2,*], Trevor J. Vincent[3,*], Sheryl L. Herrera[1] and Melanie Martin[1-3]

[1]Department of Physics and Astronomy, University of Manitoba, [2]Department of Radiology, University of Manitoba, [3]Department of Physics, University of Winnipeg. *Co-first authors. Corresponding author email: m.martin@uwinnipeg.ca

**Abstract:** MRI and Monte Carlo simulated data of pulsed gradient spin echo experiments were used to study the effects of diffusion time, gradient strength and b-value on diffusion tensor (DT) metrics using real and simulated fixed rat spines. Radial ($\lambda_\perp$) in grey matter and simulation data, axial ($\lambda_\parallel$) in both grey and white matter in fixed rat spinal cords and mean diffusivity in all tissues showed a significant decrease with diffusion time at b = 1 $\mu m^2$/ms. All diffusivities significantly decreased with b-value at g = 116 mT/m and at $\Delta_{eff}$ = 23 ms. The fractional anisotropy (FA) significantly increased with diffusion time at b = 1 $\mu m^2$/ms in the simulation data and grey matter. FA significantly increased in white matter and simulation data and significantly decreased in grey matter with b-value at g = 116 mT/m and at $\Delta_{eff}$ = 23 ms. These data suggest that DTI metrics are highly dependent on pulse sequence parameters.

**Keywords:** diffusion, diffusion time, diffusion tensor, rat, spine, b-value, gradient strength

This article is available from http://www.la-press.com.

# Introduction

The advent of diffusion tensor (DT) magnetic resonance (MR) imaging has made a significant impact in the field of neuroimaging.[1–9] Many different metrics can be calculated from DTI and can be used to infer information about the underlying microstructural features of the tissue in each voxel. Mean diffusivity (MD), fractional anisotropy (FA), and axial ($\lambda_{\parallel}$) and radial ($\lambda_{\perp}$) diffusivities have been shown to change with disease, damage or dysfunction,[9–13] as well as development[5,14–19] and aging[20,21] in the brain.

Signal from a diffusion pulse sequence, such as the Stejskal-Tanner pulsed gradient spin echo (PGSE) sequence,[22] is attenuated by a factor $e^{-bADC}$, where ADC is the apparent diffusion coefficient of water in the voxel and b depends on the pulse sequence used and its parameters, including those relating to gradient pulses. Thus, in a simple diffusion-weighted imaging experiment, one can acquire a signal without much diffusion weighting where b is close to zero, and one can also acquire a signal with diffusion weighting where b is non-zero. Assuming the signal decay is mono-exponential, one can easily calculate the ADC.

The measured ADC of water in tissue can be dependent on the diffusion-gradient direction because of the anisotropic nature of tissue.[5–7,9,23] Cellular structures can hinder or restrict water diffusion, causing the measured ADC to be smaller than the free diffusion coefficient. The hindrance can have different effects in different directions depending on the presence of cellular structures and their permeability to water molecules. Thus, DTI measurements combine several diffusion-weighted sequences in at least six different directions to measure the diffusion tensor.

Many groups use several gradient directions and a single b-value per direction to do DTI calculations, because it has been shown that at least 30 unique and evenly distributed gradient orientations are needed for robust determination of many DTI metrics.[24] It has been shown that the diffusion signal and metrics of the diffusion tensor change with increasing b-value in the developing rat brain.[25] It was concluded that the capability of DTI metrics to detect axonal damage and demyelination[11,13,26–28] critically depends on the specific b-value used.[25] Thus, it was suggested that b-values be optimized for detecting specific neural tissue changes.[25]

Previous studies have shown that DTI metrics change with b-value, using constant timings and different gradient strengths.[25] Diffusion signal is also diffusion time dependent,[29–41] and thus changing the diffusion time can affect the non-mono-exponential decay behavior.

The effects of diffusion time on DTI metrics are controversial.[42] Some studies indicated that white matter DTI metrics were basically unchanged for diffusion times ranging from 8 to 2000 ms.[43–46] Other studies found changes with diffusion time.[38,40,41] It has been proposed that shorter diffusion times affect DTI metrics.[47,48] Preliminary studies of rat brain support this proposal.[49] DTI metrics could also be diffusion gradient strength-dependent. Measurements made at constant b-values but with different diffusion times and diffusion gradient strengths also showed changes.[38] It was suggested[38] this decrease was not seen by others[43] because of the use of constant b-values. Data were acquired with constant gradient strength, but while careful attention was paid to the diffusion pulse sequence parameters, the echo time ranged from 67.9 to 96.9 ms.[38] Thus, the observed changes could be due to $T_2$ rather than diffusion effects. A more comprehensive study is needed to characterize the effect of diffusion time on DTI metrics in CNS tissue.

Here we use Monte Carlo computer simulations to show the effects of diffusion time on DT metrics (MD, FA, $\lambda_{\parallel}$, and $\lambda_{\perp}$) using two different geometries. The first geometry consisted of square cylinders on a square lattice[29] and the second geometry consisted of cylinders on a hexagonal lattice.[47] We used three gradient directions: one along the cylinders, corresponding to the direction of the axial diffusivity, and two perpendicular to this direction, whose results can be averaged to correspond to the direction of the radial diffusivity. The effects of using two diffusion images, one with low b-value close to zero and the other with high b-value, each with different diffusion times, were also studied. We also measured the effects of diffusion time on DT metrics using fixed rat spines for comparisons with the simulation data.

## Methods
### Sample preparation
Two healthy adult rats were sacrificed using transcardiac perfusion. Under isoflurane anesthetic, phosphate-buffered saline (PBS) solution was injected

into the left ventricle of the heart for 10 minutes, followed by 4% paraformaldehyde (PFA) in 0.1 M PBS (pH 7.6). Spinal cords were excised and fixed in 4% PFA for one week. Prior to imaging, spinal cords were washed in 0.1 M PBS for 48 hours to remove any excess fixative. After washing, two thoracic spinal cord sections were wrapped together with Teflon tape along with an NMR glass containing 0.1 M PBS solution capped on both ends with paraffin wax. Teflon tape was wrapped around both ends of the sample to hold it firmly in a 50 mL plastic sample tube. The tube was filled with room temperature Fomblin® Perfluoropolyether Y04 grade fluid (Solvay Solexis) to eliminate external proton signal and susceptibility artifacts and maintain moisture in the samples. The sample holder was left at room temperature for several hours to allow the sample temperature to equilibrate.

## Imaging

The sample tube was placed in a custom-built 33 mm inductively-coupled quadrature RF volume coil (NRC Institute for Biodiagnostics, Winnipeg, MB, Canada) and maintained at 20 °C ± 2 °C during imaging. All MR experiments were performed on a 7 T 21 cm Bruker Avance III NMR system with a BGA12-S actively-shielded gradient system and Paravision 5.

Three 1 mm thick slices, spaced 3 mm apart, were placed perpendicular to the two spinal cords and the PBS sample. All acquisitions had an FOV of $3 \times 3$ cm and a $256 \times 256$ matrix size for an in-plane resolution of $117 \times 117$ $\mu m^2$. DTI data were acquired with a PGSE sequence using a 6-direction icosahedral gradient encoding scheme. In order to accommodate a large range of diffusion times and reduce the effect of $T_2$ relaxation, TE was held constant at 75 ms. TR = 1500 ms and gradient pulse duration, $\delta = 4.5$ ms. The low b-value was 0.00123 ms/$\mu m^2$ and the high b-value ranged from 0.979 to 1.002 ms/$\mu m^2$ depending on gradient direction. Fat suppression was turned on to reduce chemical shift artifacts and the readout bandwidth was relatively low (12.5 kHz) to improve SNR.

For the first set of experiments, eight different gradient separation times were logarithmically spaced between 8 and 56.5 ms ($\Delta = 8$, 10.5, 14, 18.5, 24.5, 32.5, 42.5, and 56.5 ms). At $\Delta = 8$ ms, the gradient strength was 352 mT/m to achieve b = 1 ms/$\mu m^2$, but

only 116 mT/m at $\Delta = 56.5$ ms. The effective diffusion times are $\Delta - \delta/3 = 6.5$, 9, 12.5, 17, 23, 31, 41, and 55 ms. Each DTI experiment was acquired with 8 averages for a total acquisition time of 6 hours × 8 experiments = 48 hours.

Given the skepticism about previous measurements, because the changing gradient strength might affect the DTI metrics, a second set of experiments were used to compare DTI metrics as a function of diffusion time by keeping the gradient strength (g = 116 mT/m) and gradient pulse duration ($\delta = 4.5$ ms) constant while varying $\Delta = 8$, 10.5, 14, 18.5, 24.5, 32.5, 42.5, 56.5 ms and thus b = 0.10878, 0.15472, 0.21904, 0.30173, 0.41198, 0.55899, 0.74274, 1.000 ms/$\mu m^2$. To keep the signal-to-noise ratio (SNR) similar in all measurements, the signal loss due to the different b-factors was calculated assuming an ADC of 0.5 $\mu m^2$/ms and the minimum number of averages to increase the SNR to at least that of the highest b-factor image with 8 averages was used. Thus, the numbers of averages used in these measurements were 4, 4, 4, 4, 5, 6, 7, and 8 for a total acquisition time of 31.5 hours.

Another set of experiments was run to assess the effect of changing gradient strength without changing the diffusion time. Images were acquired with constant $\Delta = 24.5$ ms, $\delta = 4.5$ ms and varying g = 59.6, 71.0, 84.5, 99.2, 116, 135, 156, 181 mT/m corresponding to the same b-values as in the second experiment, namely b = 0.10878, 0.15472, 0.21904, 0.30173, 0.41198, 0.55899, 0.74274, 1.000 ms/$\mu m^2$. Again, to keep the SNR similar in all measurements, the signal loss due to the different b-factors was calculated assuming an ADC of 0.5 $\mu m^2$/ms and the minimum number of averages to increase the SNR to at least that of the highest b-factor image with 8 averages was used. Thus, the numbers of averages used in these measurements were 4, 4, 4, 4, 5, 6, 7, and 8 for a total acquisition time of 31.5 hours.

Using a custom-built MATLAB tool, all images from each experiment were registered to the low b-value image for that experiment or the lowest $\Delta$ for the first experiment. The registration used a rigid affine transformation matrix determined automatically by maximizing the 2D correlation coefficient between the two images. An anisotropic diffusion filter was subsequently applied to improve the apparent SNR.[50,51] The filter was applied with 3 iterations and a gradient

modulus threshold equal to three times the standard deviation of the noise in each image.[52] Diffusion tensors were determined using a non-linear least-squares fit and a modified Cholesky decomposition to ensure positive definiteness.[53] After diagonalization, DTI metric maps (FA, MD, $\lambda_{\parallel}$ and $\lambda$) were calculated. Thirty-nine regions of interest (ROIs) were defined in the images, 13 per slice, including the left, right, ventral, and dorsal regions of the white matter and the left and right regions of the grey matter of the spinal cords as well as the PBS sample as shown in Figure 1.

## Monte Carlo simulation

A Monte Carlo computer simulation of the experiments was conducted. The simulation was programmed in C++ following a previously used method.[29] Two different geometries were used to simulate tissues similar to white matter in rat spines as previously described.[47]

The first geometry consisted of 5.35 μm parallel square cylinders defined on a square lattice with a 6.02 μm spacing and a packing fraction of f = 0.79. The geometry for the second simulation consisted of 5.35-μm diameter parallel cylinders defined on a hexagonal lattice with a packing of f = 0.79.
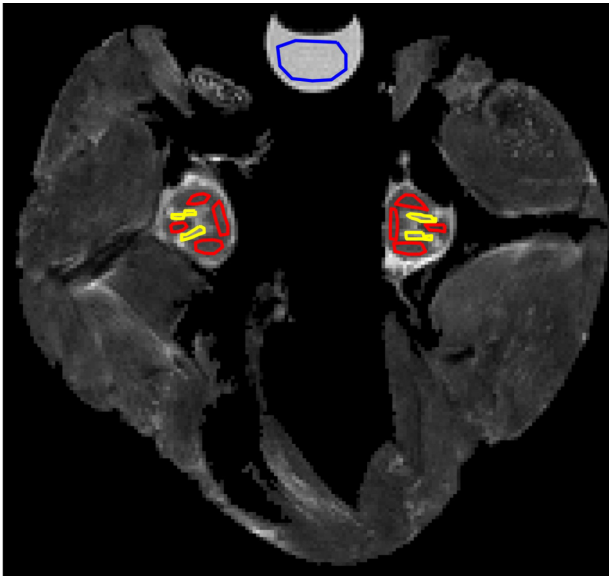


**Figure 1.** Thirteen regions of interest (ROIs) selected in one image slice of two rat spines.
**Notes:** The left, right, ventral, and dorsal regions of the white matter are outlined in red. The left and right regions of the grey matter are outlined in yellow. The PBS ROI is outlined in blue. Similar ROIs were selected in the other two slices.

Intracellular space was defined as the interior of the cylinders and extracellular space was defined as exterior to the cylinders. The intracellular and extracellular spaces were associated with distinct diffusion coefficients. For all simulations, $D_i = 1.0$ μm²/ms and $D_e = 2.5$ μm²/ms and the $T_2$ relaxation times were homogenous.[29]

A set of N = 100,000 point particles was uniformly distributed in a random manner over the lattice. At each time step of 1 μs, the position of a particle was updated by generating a step vector with a random orientation in 3-dimensional space. The magnitude of the step vector was determined by the product of the speed of the particle and the length of the time step. The speed was calculated using $v = \sqrt{6D/\delta t}$, where D is the diffusion coefficient of the space containing the particle, and $\delta t$ is the length of the time step.

If the point particle reached a boundary, it would be specularly reflected because, for this simulation, the permeability of the barriers was set to 0. The simulation allowed for multiple reflections in a single time step.

The simulation modeled a PGSE sequence to derive the ADC from the spin magnetization vectors of the particles. The transverse component of the spin magnetization vector, $M_{\perp}$, was stored for each particle and tracked over the particle's trajectory. Before the starting time t = 0, the $M_{\perp}$ for the ith particle, $M_{i\perp} = (m_{xi}, m_{yi})$, was assigned the value (1, 0). This assignment modeled the alignment of the magnetization vectors by a 90° RF pulse in the -y-direction. The rest of the simulated sequence consisted of two bipolar gradients.

During a time step in which a gradient was being applied, $M_{\perp}$ was rotated through an angle $\delta\varphi_i$:

$$\delta\varphi_i = \gamma G(t) \cdot r_i(t)\delta t,$$

where $r_i(t)$ is the position vector of the ith particle at time $t$, $\gamma$ is the proton gyromagnetic constant, and $G(t)$ is the gradient vector, with magnitude $G$, defined by

$$G(t) = \begin{cases} G\widehat{G} & 0 \le t \le \delta \\ -G(t-\Delta)\,\widehat{G} & \Delta \le t \le \Delta + \delta, \\ 0 & otherwise \end{cases}$$

Once the echo time had elapsed, the signal of the $N$ particle ensemble was found by calculating the magnitude of the mean $M_\perp$:

$$S = \left| \frac{1}{N} \sum_i^N M_{i\perp} \right|,$$

For each signal, a corresponding b-value was obtained from the equation $b = \gamma^2 \delta^2 G^2 (\Delta - \delta/3)$. The ADC was then calculated through linear regression of the [b, lnS(b)] data points.

Pulse sequence parameters, including echo times and diffusion gradients and timings, were made to match the parameters from the imaged spines.

In addition, the simulation data were used to fit lnS(b) to b using two data points, one at b = 0.10878 ms/µm² and one with b = 1 ms/µm². Several pairs of b-values were used. For each of the b-values, $\Delta$ was one of eight possible values; 8, 10.5, 14, 18.5, 24.5, 32.5, 42.5, and 56.5 ms. Thus 64 fits of lnS(b) to b using two data points, one at b = 0.10878 ms/µm² and one with b = 1 ms/µm², were used to calculate the ADC value for the simulation. If $\Delta$ had no effect on ADC then presumably each fit would give an identical value, given that the fits were using identical values for b.

## Statistical analysis

To determine whether there were statistically significant changes in DTI metrics with diffusion time or b-value, statistics were performed using SAS® 9.2 software. One-way ANOVAs were used to measure the significance in the effects of effective diffusion times and b-values on the diffusion tensor metrics (FA, MD, $\lambda_\parallel$ and $\lambda_\perp$) using real and simulated fixed rat spines. One-way ANOVAs were also used to measure the significance of effective diffusion time on diffusion tensor metrics when two different effective diffusion times were used in the fit to calculate the diffusion tensor. Statistical significance was determined using a threshold value of 0.05, where any $P$-values less than 0.05 would indicate a statistically significant difference.

## Results

$\lambda_\parallel$, $\lambda_\perp$ and MD were calculated from the simulation data and from the rat spine images and are plotted in Figure 2. Significant variations in these data were

confirmed with one-way ANOVAs, with $P$-values much less than 0.0001. As shown in Figure 2A, axial diffusivity decreased significantly with effective diffusion time and constant b-value in both white matter and grey matter; however, it did not show any significant change in the simulated data. Also shown in Figure 2A, radial diffusivity decreased significantly with effective diffusion time and constant b-value in both the simulated data and in grey matter. No significant change was detected in white matter. Mean diffusivity showed significant decreases in the simulated data, as well as in white matter and grey matter. In both the simulation and experimental data, all diffusivities significantly decreased with diffusion time when gradient strength was held constant, as shown in Figure 2B, and with b-value when diffusion time was held constant, as shown in Figure 2C. The differences between diffusion metrics in white matter and grey matter were also dependent on effective diffusion time, b-value and gradient strength.

FA values were calculated from these data and are plotted in Figure 3. The significant variations in these data were confirmed with one-way ANOVA, with $P$-values much less than 0.0001. As shown in Figure 3A, FA values significantly increased with diffusion time and constant b-value in the simulation data as well as in grey matter, however no variation was detected in FA values of white matter. Smaller significant increases were detected in FA with diffusion time when g was held constant, as shown in Figure 3B, and with b-value when diffusion time was held constant, as shown in Figure 3C, in both the simulation data and white matter. However, a significant decrease was detected in FA in grey matter with b-value when gradient strength or effective-diffusion time was held constant. The difference between FA values in white matter and grey matter depends on diffusion time, gradient strength, and b-value, with greater differences occurring for larger b-values and effective diffusion times. A summary of the changes in $\lambda_\parallel$, $\lambda_\perp$, MD and FA with (a) $\Delta$ and g at constant b, (b) $\Delta$ and b at constant g, and (c) b and g at constant $\Delta$ are given in Table 1.

The diffusivities and FA values calculated using two data points, one with b = 0.10878 ms/µm² and one with b = 1 ms/µm², are shown in Figure 4. The significant variations in these data were confirmed with one-way ANOVA, with $P$-values much less than 0.0001.
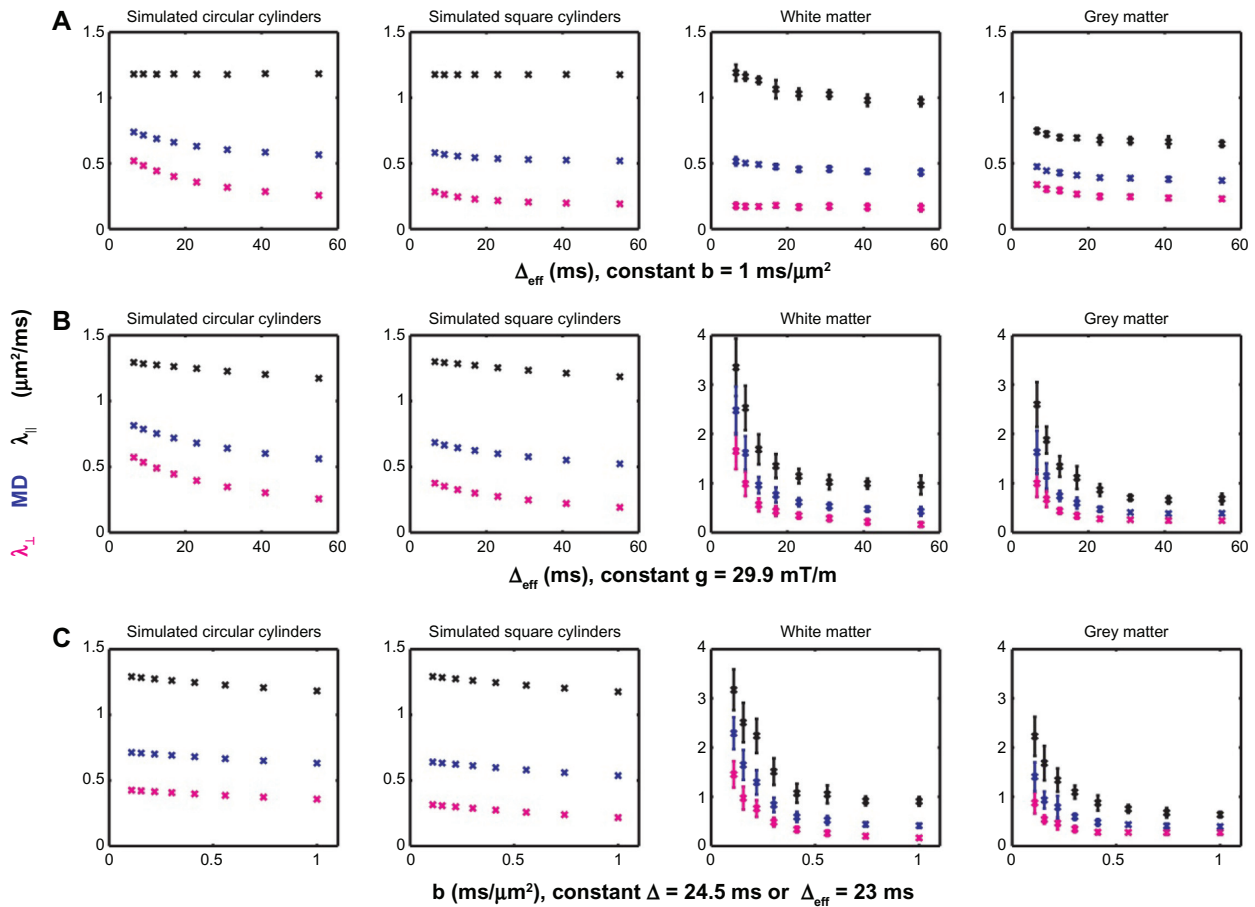
**Figure 2.** Axial ($\lambda_{\parallel}$) shown in black, radial ($\lambda_{\perp}$), shown in magenta, and mean (MD), shown in blue, diffusivities calculated from simulation data for square cylinders (first column), circular cylinders (second column) and from rat spine white matter (third column) and grey matter (fourth column). Note that the vertical axis scale changes for the rat spine data. Error bars for the simulation data are calculated from standard deviations in the diffusion tensor eigenvalues from three different runs of the simulation. Errors in the rat data are the standard deviations of the parameters in the ROIs. (**A**) These data were collected from experiments with constant b = 1 ms/µm² and plotted versus effective diffusion-time ($\Delta_{eff}$). (**B**) These data were collected from experiments with constant g = 29.9 mT/m and plotted versus $\Delta_{eff}$. (**C**) These data were collected from experiments with constant $\Delta$ = 24.5 ms and plotted versus b-value.
**Notes:** With diffusion time, $\lambda_{\parallel}$ significantly decreases in white and grey matter, $\lambda_{\perp}$ significantly decreases in the simulation data and in grey matter, and MD significantly decreases in both simulation data and white and grey matter, when b is held constant. All diffusivities significantly decrease with b-value when g or effective diffusion time is held constant. Note that at different values of $\Delta_{eff}$ and b, the difference between white matter and grey matter diffusivities changes.

The red line represents the "true" metric values calculated from two data points with identical effective diffusion times, and are similar to the graphs shown in the first row of Figures 1 and 2. No significant change in any of the DTI metrics was detected with effective diffusion time when comparing the means of all the measurements (P-values all greater than 0.05).

## Discussion

Simulation data show significant decreases with effective diffusion time at constant b-value ($\lambda_{\perp}$, MD) and at constant gradient strength ($\lambda_{\parallel}$, $\lambda_{\perp}$, MD) similar to some studies[29–41] and differing from others.[25,43–46] Previous studies have suggested that missing changes are due to having a constant b-value instead of

constant gradient strength, which does not appear to be the case for these simulation data. Therefore, this lack of change in previously collected data could be due to $T_2$ effects.[38] Significant decreases in DT metrics were detected at $\Delta_{eff}$ of 23 ms, similar to previous studies that showed significant changes in DT metrics in developing rat brains with b-value at $\Delta_{eff}$ of 15.3 and 18.3 ms.[25]

$\lambda_{\parallel}$ and MD in both white and grey matter in fixed rat spinal cords, and $\lambda_{\perp}$ in only grey matter in the fixed spinal cords, significantly decreased with effective diffusion time at b = 1 µm²/ms. The noise in these data, as well as partial volume averaging effects, could account for the difference detected between the data and simulation. Also, a two-compartment model
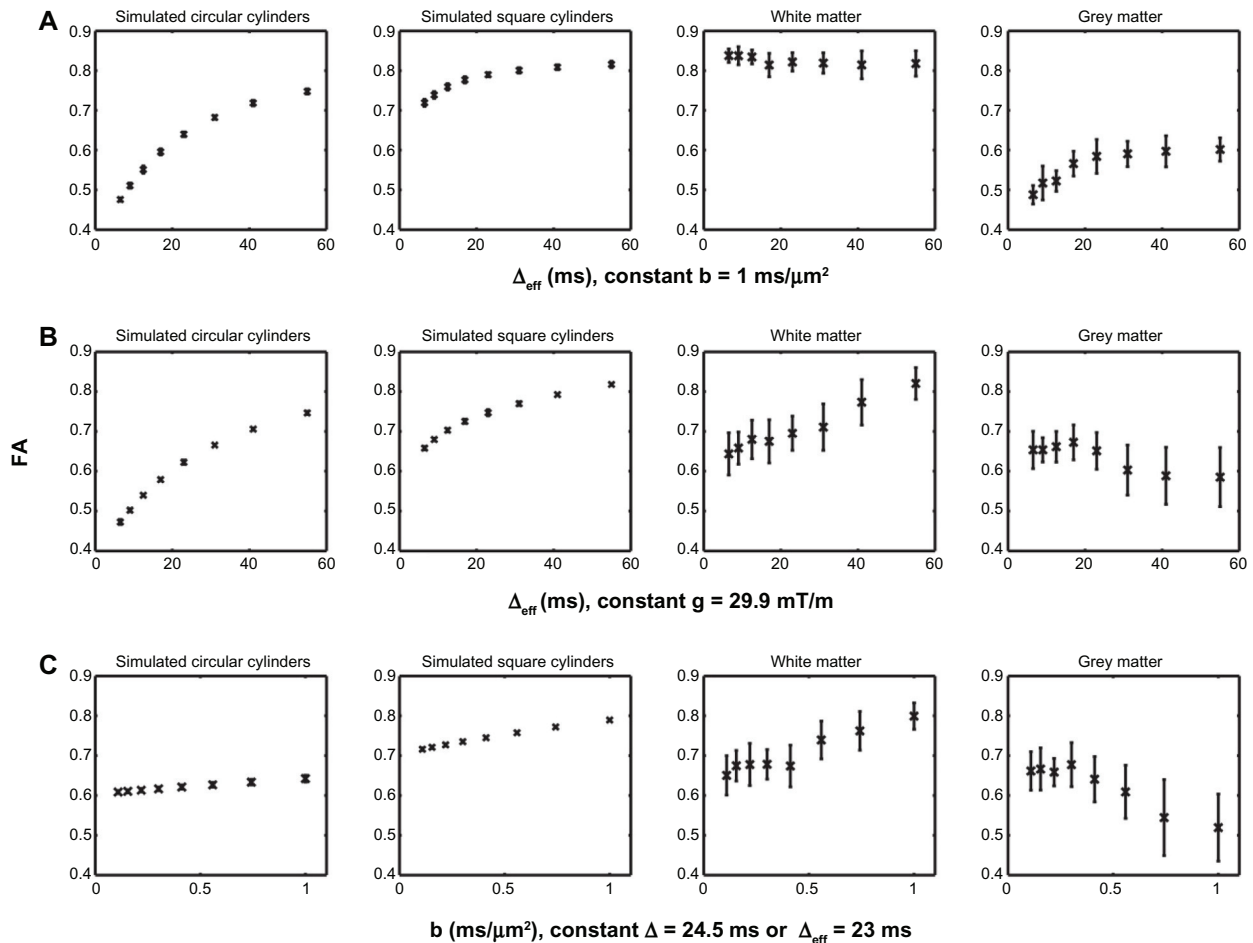
**Figure 3.** Fractional anisotropies calculated from simulation data for square cylinders (first column), circular cylinders (second column) and from rat spine white matter (third column) and grey matter (fourth column). Error bars for the simulation data are calculated standard deviations in the diffusion tensor eigenvalues from three different runs of the simulation. Errors in the rat data are the standard deviations of the FA values in the ROIs. (**A**) These data were collected from experiments with constant b = 1 ms/μm² and plotted versus $\Delta_{eff}$. (**B**) These data were collected from experiments with constant g = 29.9 mT/m and plotted versus $\Delta_{eff}$. (**C**) These data were collected from experiments with constant $\Delta$ = 24.5 ms and plotted versus b-value.
**Notes:** FA significantly increased in simulation data in all plots. In grey matter, FA significantly increased with effective diffusion-time when b was held constant and decreased with b-value when gradient strength or effective diffusion-time was held constant. In white matter, FA significantly increased only with b-value when gradient strength or effective diffusion-time was held constant. The difference between FA values measured in white matter and grey matter, is also dependent on b, g and $\Delta_{eff}$.

with constant diffusion coefficients for each compartment might be an oversimplification of the tissue. Nonetheless, the data do agree with some previous studies.[25,43–46]

All diffusivities measured in both grey and white matter significantly decreased with b-value when gradient strength or effective diffusion time was held constant. The difference in parameter values between grey and white matter also varied when gradient strength or effective diffusion time was held constant.

Increases were observed in FA with effective diffusion time, when b or g was held constant in the simulation data. Smaller increases were observed in FA with b when the effective diffusion time was held constant.

These data clearly indicate that for tissue with similar properties to those simulated, FA values are diffusion time-dependent.

In white matter, no change in FA was detected when effective diffusion time varied at b = 1 μm²/ms. A significant increase was detected in FA in white matter with b-value when diffusion time or gradient strength was held constant. In grey matter, an increase was detected in FA with diffusion time when b was held constant and a decrease was detected in FA with b-value when gradient strength or diffusion time was held constant. These data suggest that FA is highly dependent on pulse sequence parameters. The contrast in FA maps between white matter and grey matter is also highly dependent on pulse sequence parameters.

**Table 1** Summary of changes detected in diffusion tensor metrics in different simulation geometries and different tissues. Many diffusivities decreased with increasing b value, gradient strength, and/or diffusion time. Fractional anisotropy increased with b value, gradient strength, and diffusion time in all simulated tissues. In white matter, FA increased with gradient strength, and diffusion time. In grey matter, FA decreased with b-value, gradient strength, and diffusion time.

| | Circular Cylinders | Square Cylinders | White Matter | Grey Matter |
|---|---|---|---|---|
| **a. Constant b varying $\Delta$ and g** | | | | |
| $\lambda_\parallel$ | – | – | ↓ | ↓ |
| $\lambda_\perp$ | ↓ | ↓ | – | ↓ |
| MD | ↓ | ↓ | ↓ | ↓ |
| FA | ↑ | ↑ | – | ↑ |
| **b. Constant g varying $\Delta$ and b** | | | | |
| $\lambda_\parallel$ | ↓ | ↓ | ↓ | ↓ |
| $\lambda_\perp$ | ↓ | ↓ | ↓ | ↓ |
| MD | ↓ | ↓ | ↓ | ↓ |
| FA | ↑ | ↑ | ↑ | ↓ |
| **c. Constant $\Delta$ varying b and g** | | | | |
| $\lambda_\parallel$ | ↓ | ↓ | ↓ | ↓ |
| $\lambda_\perp$ | ↓ | ↓ | ↓ | ↓ |
| MD | ↓ | ↓ | ↓ | ↓ |
| FA | ↑ | ↑ | ↑ | ↓ |

**Notes**: ↓ indicates a significant decrease with diffusion time/gradient strength/b-value; ↑ indicates a significant increase with diffusion time/gradient strength/b-value; – indicates non-significant change with diffusion time/gradient strength/b-value.

The trends of radial and mean diffusivities with diffusion time and b-value are similar between simulation data and rat spine. When b is held constant, the trend in the increase in FA is similar between simulation and grey matter. When gradient strength or effective diffusion time is held constant, the trend of increasing FA is similar in white matter and simulation data. With varying b, the experimental data again show similar trends as the simulation data for b > 0.3.

The difference between simulation data and experimental data are likely due to the mismatch in geometry and diffusion coefficients between the simulations and tissue. For instance, the simulations used
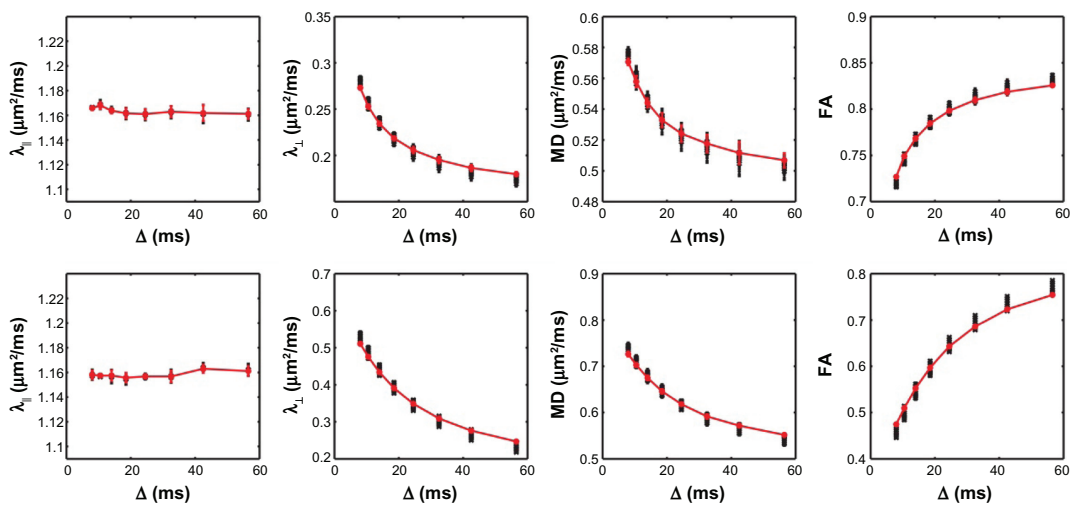


**Figure 4.** Axial ($\lambda_\parallel$) (first column), radial ($\lambda_\perp$) (second column), and mean (MD) (third column) diffusivities and FA (fourth column) calculated from simulation data for square cylinders (first row) and circular cylinders (second row) using two b-values, b = 0.10878 ms/µm² and one with b = 1 ms/µm².
**Notes:** 64 fits were performed to calculate the diffusivities and all 64 results are shown with black data points and plotted at the $\Delta$ value used for the b = 1 ms/µm² data point. The red line and data points represent the values from the fit where both b-values used identical $\Delta$ values. In contrast to Figure 1, there was no significant change in the mean value of any parameter as a function of the $\Delta$ value used for the b = 1 ms/µm² data point.

a constant diameter of 5.35 μm[47] for the cylinders, while rat spinal cord tissue has been measured to have axons that range in diameter from about 2 μm to a little more than 5 μm in diameter.[54]

One problem with the rat spine data is that the change in lnS from one b-value to the next for the first few b-values is smaller than the noise in lnS. Thus parameters measured from these data were extremely noisy. The dissimilarity between simulation and experimental data for b < 0.3 is probably because of this. Several points in the ROIs were removed from the calculations if the apparent diffusion coefficient measured from the fit was larger than 5 μm²/ms. Clearly a large SNR is required for DTI calculations, especially for small variations in b-values.

In vivo rat spinal cord measurements and simulations would add more insight into the controversies of changing DTI metrics. At body temperature all diffusion coefficients should be much larger than those at the temperatures used and simulated for the fixed spines in this study.[55] Thus, water molecules would diffuse longer distances in vivo than ex vivo. Therefore, it is less likely that DTI metrics would change with the longer diffusion times used in this study. Shorter diffusion times using oscillating gradient techniques[30] might be needed to detect changes in DTI metrics with diffusion times.

Using the 64 fits in each set of simulation data, no significant change in any of the DTI metrics was detected with effective diffusion time. Yet, the similar data in Figures 1 and 2, with constant b, using the same effective diffusion time for both measurements, show significant decreases in MD and $\lambda_\perp$ and significant increases in FA. Thus variations in DTI metrics could be missed due to changes in pulse sequence parameters when making measurements. Care should be used to acquire images with the same pulse sequence parameters in all directions for comparable results.

For tissue like fixed rat spines with structures similar to what was modeled in the simulations, care should be used when calculating and comparing diffusion tensor metrics. It is not acceptable to simply use the same b-values in several experiments and compare the data. The elements that make up the b-value, namely the gradient strength and effective diffusion time, must be the same as well.

## Conclusions

This study indicates that there are variations in measurements of diffusion tensor metrics with pulse sequence parameters, including effective diffusion time, b-value and gradient strength. For measurements to be compared between studies and within studies, pulse sequence parameters should be the same in each study. It is not sufficient to use the same b-value to compare data. Even to compare diffusion tensor metrics between studies that use the same parameters, the parameters used to obtain all b-values for all images in the study should be clearly explained.

## Competing Interests

Author(s) disclose no potential conflicts of interest.

## Author Contributions

Conceived and designed the experiments: MM, JDT, TJV. Analyzed the data: JDT, TJV, SLH, MM. Wrote the first draft of the manuscript: JDT, TJV, SLH, MM. All authors reviewed and approved of the final manuscript.

## Disclosures and Ethics

As a requirement of publication author(s) have provided to the publisher signed confirmation of compliance with legal and ethical obligations including but not limited to the following: authorship and contributorship, conflicts of interest, privacy and confidentiality and (where applicable) protection of human and animal research subjects. The authors have read and confirmed their agreement with the ICMJE authorship and conflict of interest criteria. The authors have also confirmed that this article is unique and not under consideration or published in any other publication, and that they have permission from rights holders to reproduce any copyrighted material. Any disclosures are made in

this section. The external blind peer reviewers report no conflicts of interest.

# References

1. Basser PJ, Mattiello J, LeBihan D. MR Diffusion tensor spectroscopy and imaging. *Biophys J*. 1994;66(1):259–67.
2. Basser PJ, Mattiello J, LeBihan D. Estimation of the effective self-diffusion tensor from the NMR spin echo. *J Magn Reson B*. 1994;103(3):399–412.
3. Mattiello J, Basser PJ, LeBihan D. Analytical expressions for the b-matrix in NMR diffusion imaging and spectroscopy. *J Magn Reson A*. 1994;108:131–41.
4. Basser PJ. Inferring microstructural features and the physiological state of tissues from diffusion-weighted images. *NMR Biomed*. 1995;8(7–8):333–44.
5. Basser PJ, Pierpaoli C. Microstructural and physiological features of tissues elucidated by quantitative-diffusion-tensor MRI. *J Magn Reson B*. 1996;111:209–19.
6. Pierpaoli C, Jezzard P, Basser PJ, Barnett A, Di Chiro G. Diffusion tensor MR imaging of the human brain. *Radiology*. 1996;201:637–48.
7. Pierpaoli C, Basser PJ. Toward a quantitative assessment of diffusion anisotropy. *Magn Reson Med*. 1996;36(6):893–906. Erratum in: *Magn Reson Med*. 1997;37(6):972.
8. Basser PJ, Pierpaoli C. A simplified method to measure the diffusion tensor from seven MR images. *Magn Reson Med*. 1998;39(6):928–34.
9. Le Bihan D, Mangin JF, Poupon C, et al. Diffusion tensor imaging: concepts and applications. *J Magn Reson Imaging*. 2001;13(4):534–46.
10. Werring DJ, Clark CA, Barker GJ, et al. The structural and functional mechanisms of motor recovery: complementary use of diffusion tensor and functional magnetic resonance imaging in a traumatic injury of the internal capsule. *J Neurol Neurosurg Psychiatry*. 1998;65(6):863–9.
11. Song SK, Sun SW, Ju WK, Lin SJ, Cross AH, Neufeld AH. Diffusion tensor imaging detects and differentiates axon and myelin degeneration in mouse optic nerve after retinal ischemia. *NeuroImage*. 2003;20(3):1714–22.
12. Nair G, Tanahashi Y, Low HP, Billings-Gagliardi S, Schwartz WJ, Duong TQ. Myelination and long diffusion times alter diffusion-tensor-imaging contrast in myelin-deficient shiverer mice. *Neuro Image*. 2005;28(1):165–74.
13. Sun SW, Liang HF, Trinkaus K, Cross AH, Armstrong RC, Song SK. Noninvasive Detection of cuprizone induced axonal damage and demyelination in the mouse corpus callosum. *Magn Reson Med*. 2006;55(2):302–8.
14. Hüppi PS, Maier SE, Peled S, et al. Microstructural development of human newborn cerebral white matter assessed in vivo by diffusion tensor magnetic resonance imaging. *Pediatr Res*. 1998;44(4):584–90.
15. Baratti C, Barnett AS, Pierpaoli C. Comparative MR imaging study of brain maturation in kittens with T1, T2, and the trace of the diffusion tensor. *Radiology*. 1999;210(1):133–42.
16. Klingberg T, Vaidya CJ, Gabrieli JD, Moseley ME, Hedehus M. Myelination and organization of the frontal white matter in children: a diffusion tensor MRI study. *Neuroreport*. 1999;10(13):2817–21.
17. Rivkin, MJ. Developmental neuroimaging of children using magnetic resonance techniques. *Ment Retard Dev Disabil Res Rev*. 2000;6(1):68–80.
18. Paus T, Collins DL, Evans AC, Leonard G, Pike B, Zijdenbos A. Maturation of white matter in the human brain: a review of magnetic resonance studies. *Brain Res Bull*. 2001;54(3):255–66.
19. Feldman HM, Yeatman JD, Lee ES, Barde, LH, Gaman-Bean, S. Diffusion tensor imaging: a review for pediatric researchers and clinicians. *J Dev Behav Pediatr*. 2010;31(4):346–56.
20. Salthouse, TA. Neuroanatomical substrates of age-related cognitive decline. *Psychol Bull*. 2011;137(5):753–84.
21. Moseley, M. Diffusion tensor imaging and aging—a review. *NMR Biomed*. 2002;15(7–8):553–60.
22. Stejskal EO, Tanner JE. Spin diffusion measurements: Spin echoes in the presence of a time-dependent field gradient. *J Chem Phys*. 1965;42:288–92.
23. Beaulieu C. The basis of anisotropic water diffusion in the nervous system—a technical review. *NMR Biomed*. 2002;15(7–8):435–55.
24. Jones DK. The effect of gradient sampling schemes on measures derived from diffusion tensor MRI: a Monte Carlo Study. *Magn Reson Med*. 2004;51(4):807–15.
25. Hui ES, Cheung MM, Chan KC, Wu EX. B-value dependence of DTI quantitation and sensitivity in detecting neural tissue changes. *Neuroimage*. 2010;49(3):2366–74.
26. Kolbe S, Chapman C, Nguyen T, et al. Optic nerve diffusion changes and atrophy jointly predict visual dysfunction after optic neuritis. *Neuroimage*. 2009;45(3):679–86.
27. Roosendaal SD, Geurts JJ, Vrenken H, et al. Regional DTI differences in multiple sclerosis patients. *Neuroimage*. 2009;44(4):1397–403.
28. Song SK, Sun SW, Ramsbottom MJ, Chang C, Russell J, Cross AH. Dysmyelination revealed through MRI as increased radial (but unchanged axial) diffusion of water. *Neuroimage*. 2002;17(3):1429–36.
29. Szafer A, Zhong J, Gore JC. Theoretical model for water diffusion in tissues. *Magn Reson Med*. 1995;33(5):697–712.
30. Schachter M, Does MD, Anderson AW, Gore JC. Measurements of restricted diffusion using an oscillating gradient spin-echo sequence. *J Magn Reson*. 2000;147(2):233–7.
31. Mitra PP, Sen PN. Effects of microgeometry and surface relaxation on NMR pulsed-field-gradient experiments: Simple pore geometries. *Phys Rev B Condens Matter*. 1992;45(1):143–56.
32. Mitra PP, Sen PN, Schwartz LM, Le Doussal P. Diffusion propagator as a probe of the structure of porous media. *Phys Rev Lett*. 1992;68(24):3555–8.
33. Latour LL, Mitra PP, Kleinberg RL, Sotak CH. Time dependent diffusion coefficient of fluids in porous media as a probe to surface-to-volume ratio. *Journal of Magnetic Resonance*. 1993;101(3):342–6.
34. Mitra PP, Sen PN, Schwartz LM. Short-time behavior of the diffusion coefficient as a geometrical probe of porous media. *Phys Rev B Condens Matter*. 1993;47(14):8565–74.
35. Latour LL, Svoboda K, Mitra PP, Sotak CH. Time-dependent diffusion of water in a biological model system. *Proc Natl Acad Sci U S A*. 1994;91(4):1229–33.
36. Meier C, Dreher W, Leibfritz D. Diffusion in Compartmental Systems. I. A comparison of an analytical model with simulations. *Magn Reson Med*. 2003;50(3):500–9.
37. Kim S, Chi-Fishman G, Barnett AS, Pierpaoli C. Dependence on diffusion time of apparent diffusion tensor of ex vivo calf tongue and heart. *Magn Reson Med*. 2005;54(6):1387–96.
38. Gao S, Wang XY, Bao SL. Effects of diffusion-time and diffusion gradient strength on the mean diffusivity of water molecules in healthy human brain. *Progress in Natural Science*. 2006;16(7):706–11.
39. Nilsson M, Lätt J, Nordh E, Wirestam R, Ståhlberg F, Brockstedt S. On the effects of a varied diffusion time in vivo: is the diffusion in white matter restricted? *Magn Reson Imaging*. 2009;27(2):176–87.
40. Horsfield MA, Barker GJ, McDonald WI. Self-diffusion in CNS tissue by volume-selective proton NMR. *Magn Reson Med*. 1994;31(6):637–44.
41. Assaf Y, Cohen Y. Non-mono-exponential attenuation of water and N-acetyl aspartate signals due to diffusion in brain tissue. *J Magn Reson*. 1998;131(1):69–85.
42. Norris DG. The effects of microscopic tissue parameters on the diffusion weighted magnetic resonance imaging experiment. *NMR Biomed*. 2001;14(2):77–93.
43. Clark CA, Hedehus M, Moseley ME. Diffusion time dependence of the apparent diffusion tensor in healthy human brain and white matter disease. *Magn Reson Med*. 2001;45(6):1126–9.
44. Le Bihan D, Turner R, Douek P. Is water diffusion restricted in human brain white-matter? An echo-planar NMR imaging study. *Neuroreport*. 1993;4(7):887–90.
45. van Gelderen P, de Vleeschouwer MH, DesPres D, Pekar J, van Zijl PCM, Moonen CT. Water diffusion and acute stroke. *Magn Reson Med*. 1994;31(2):154–63.
46. Niendorf T, Dijkhuizen RM, Norris DG, van Lookeren Campagne M, Nicolay K. Biexponential diffusion attenuation in various states of brain tissue: implications for diffusion-weighted imaging. *Magn Reson Med*. 1996;36(6):847–57.

47. Ford JC, Hackney DB, Lavi E, Phillips M, Patel U. Dependence of apparent diffusion coefficients on axonal spacing, membrane permeability, and diffusion time in spinal cord white matter. *J Magn Reson Imaging*. 1998; 8(4):775–82.

48. Gore JC, Xu J, Colvin DC, Yankeelov TE, Parsons EC, Does MD. Characterization of tissue structure at varying length scales using temporal diffusion spectroscopy. *NMR Biomed*. 2010;23(7):745–56.

49. Kershaw J, Leuze C, Obata T, Kanno I, Aoki I. Changes to the fractional anisotropy and mean diffusivity of in vivo rat brain measured at short effective diffusion-times. *Proc Intl Soc Mag Reson Med*. 2011;19:409.

50. Perona P, Malik J. Scale-space and edge detection using anisotropic diffusion. *IEEE Transactions on Pattern Analysis and Machine Intelligence*. 1990;12(7):629–39.

51. Gerig G, Kubler O, Kikinis R, Jolesz FA. Nonlinear anisotropic filtering of MRI data. *IEEE Trans Med Imaging*. 1992;11(2):221–32.

52. Jones CK, Whittall KP, MacKay AL. Robust myelin water quantification: averaging vs. spatial filtering. *Magn Reson Med*. 2003;50(1):206–9.

53. Koay CG, Chang LC, Carew JD, Pierpaoli C, Basser PJ. A unifying theoretical and algorithmic framework for least squares methods of estimation in diffusion tensor imaging. *J Magn Reson*. 2006;182(1):115–25.

54. Dula AN, Gochberg DF, Valentine HL, Valentine WM, Does MD. Multiexponential T2, magnetization transfer, and quantitative histology in white matter tracts of rat spinal cord. *Magn Reson Med*. 2010;63(4):902–9.

55. Rane S, Duong TQ. Comparison of in vivo and ex vivo diffusion tensor imaging in rhesus macaques at short and long diffusion times. *Open Neuroimag J*. 2011;5:172–8.